Factors influencing the skill of synthesized satellite wind products in the tropical Pacific.

Shayne McGregor[1,2], Alex Sen Gupta[2,3], Dietmar Dommenget[1,2], Tony Lee[4], Michael J. McPhaden[5] and William S. Kessler[5].

[1] School of Earth, Atmosphere and Environment, Monash University, Clayton, Victoria, Australia.
[2] ARC Centre of Excellence for Climate System Science, Australia.
[3] Climate Change Research Centre, University of New South Wales, Sydney, Australia.
[4] Jet Propulsion Laboratory, California Institute of Technology, Pasadena, California, USA
[5] Pacific Marine Environmental Laboratory, NOAA, Seattle, Washington, USA

Submitted to JGR oceans 16th September 2016; revised 24th November 2016.

Abstract

Given the importance of tropical Pacific winds to global climate, it is interesting to examine differences in the mean and trend among various wind products, and their implications for ocean circulation. Past analysis has revealed that despite the assimilation of observational data, there remain large differences among reanalysis products. Thus, here we examine if satellite-based synthesis products may provide more consistent estimate than reanalysis. Reanalysis product winds are, however, typically used as a background constraint in constructing the synthesis products to fill spatiotemporal gaps and to deal with satellite wind direction ambiguity. Our study identified two important factors that influence both the mean and trends from synthesized wind products. Firstly, the choice of background wind product in synthesised satellite wind products affects the mean and long-term trends, which has implications for simulations of ocean circulation, sea level, and presumably SST. Secondly, we identify a clear need for developing a better understanding of, and correcting differences between in-situ observations of absolute winds with the satellite-derived relative winds prior to synthesizing. This correction requires careful analysis of satellite surface winds with existing co-located in-situ measurements of surface winds and currents, and will benefit from near surface current observations of the proposed Tropical Pacific Observing System. These results also illustrate the difficulty in independently evaluating the synthesis wind products because the in-situ data have been utilised at numerous steps during their development. Addressing these identified issues effectively, will require enhanced collaborations among the wind observation (both satellite and in-situ), reanalysis, and synthesis communities.

1. Introduction

The primary motivation for this study is to provide timely information for the development of the Tropical Pacific Observing System (TPOS) by understanding what factors are important in determining the long term mean and linear trend in synthesised satellite wind products. Observations of ocean surface winds are important for understanding many oceanic and atmospheric processes, including ocean circulation changes, regional changes in sea surface height

and air-sea fluxes of heat, moisture momentum etc. [e.g., McPhaden et al. 1998; Timmerman et al. 2010; Sen Gupta et al. 2012; 2016]. In the tropical Pacific, ocean surface wind observations are critical for understanding the initiation and development of El Niño-Southern Oscillation (ENSO), a dominant mode of interannual climate variability [McPhaden et al. 2006].

Changes in the Pacific Trade winds have had dramatic regional and global impacts over recent decades, associated with a rapid and unprecedented (in the relatively short observational record) strengthening since the early 1990's [e.g., England et al. 2014]. This change has been related to: i) the recent hiatus in global surface warming [England et al. 2014; Kosaka and Xie 2013]; ii) the ongoing drought in California [McGregor et al. 2014]; iii) the rapid increase in western tropical Pacific sea level, with a trend three times greater than the global mean [Merrifield et al. 2011; Timmermann et al. 2010], and iv) a strengthening of the equatorial under current [Amaya et al. 2015]. As such, high-quality observations of ocean surface winds across various times scales (e.g., from diurnal to decadal) in the tropical Pacific are critical for understanding the current state of the tropical Pacific and changes to the global climate.

Of primary importance for accurate and sustained regional observations has been the tropical moored array, for which initial deployment began in the 1984 through the Tropical Atmosphere Ocean (TAO) array [McPhaden et al. 1998]. Array installation was completed in 1994, with the final configuration of the tropical Pacific Ocean network consisting of approximately 70 moored buoys [McPhaden et al. 2010]. In 2000, TAO was renamed TAO/TRITON in recognition of contributions from Japan to maintain the western portion of the array with TRITON moorings [Ando et al. 2005; McPhaden et al. 2010]. The resultant TAO/TRITON array network has a relatively coarse grid structure spanning the tropical Pacific and provides near real-time, high temporal resolution measurements of a suite of oceanic and atmospheric parameters. These measurements have been essential for the development of ENSO theory and seasonal forecast systems [e.g., McPhaden et al. 1998]. While TAO/TRITON measurements have been invaluable in

these regards, the system's relatively coarse structure has not generally allowed for the direct use of its data as forcing for ocean models and has also led to questions about the way its data were assimilated to generate reanalysis products [e.g., Josey et al. 2014].

TAO/TRITON is not the only platform to measure surface winds in the tropical Pacific, as many satellite sensors have been observing surface winds over the global ocean since July 1987 for wind speed and since 1991 for vector winds [Yu and Jin 2012]. Satellites infer surface stress from scatterometer measurements of small-scale surface roughness [e.g., Chelton and Freilich 2005]. The inferred surface stress is then translated to equivalent 10m wind (by assuming that the atmospheric boundary layer is neutrally stratified) [e.g., Chelton and Freilich 2005]. Satellite wind sensors have enabled the capabilities for broad-scale coverage and for estimating wind (stress) curl and divergence at scales not afforded by in-situ arrays. Wind measurements from satellites exhibit considerable skill in reproducing the in-situ wind observations [e.g., Mears et al. 2001; Kunkee et al., 2008]. However, it is important to note that the satellite-derived data represents surface wind estimates relative to the moving ocean surface [e.g., Kelly et al. 2001]. This can have a significant impact on wind speeds in the tropical oceans where surface currents can be of comparable magnitude to the surface winds. The quality of satellite wind retrievals from some sensors (e.g., the Ku-band sensors) is sensitive to rain, with an increased rain rate related to decreased accuracy [e.g., Atlas et al. 2011; Yu and Jin 2012] and even spurious spatial derivatives like wind stress curl [e.g., Milliff et al. 2004; O'Neill et al. 2015; Kilpatrick and Xie 2015].

A third estimate of ocean surface wind comes from atmospheric reanalysis products such as the ERA-interim reanalysis of Dee et al. 2011. Each of these reanalysis products assimilates a set of observational products, including TOA/TRITON and satellite-derived observations (input data may differ between products), into a dynamical model to provide a gridded, spatially complete product. Such reanalysis are often used as an alternative to observations for analysis or the forcing of ocean models due to the complete space-time coverage and uniform resolutions. However, despite

assimilating observational data, there are some large differences between the various reanalysis products that are especially pronounced when looking at trends and means over the last few decades [Wittenberg 2004; McGregor et al. 2012; Lee et al. 2013].

Given these discrepancies around long-term trends and means in reanalysis products, it is interesting to consider if synthesized satellite observations from various missions may provide a more consistent and reliable estimate. The synthesis of wind observations from different satellites involves a number of significant challenges [Atlas et al. 2011; Yu and Jin 2012]. Firstly, an individual satellite wind sensor has limited spatiotemporal coverage. For example, a QuikSCAT-like satellite covered approximately 60% (90%) of the global ocean twice daily (daily) [Lee et al. 2008]. Multiple satellites can improve the coverage, but full coverage is still not possible at the 6-hourly resolution, a time interval over which atmospheric reanalysis provide wind estimates. As such, in order to obtain the full spatial coverage, these synthesised satellite wind products require some form of background wind to fill missing data gaps where observations are not available. Background wind products are generally one of the analysis/reanalysis wind products, which given the across-product differences highlighted by Wittenberg [2004] and McGregor et al. [2012] raises questions over their influence in the mean and longer term trends of these synthesized products. Reanalysis (background) wind products are also used to determine wind direction when there is directional ambiguity in vector wind retrieval from satellite scatterometers or when directional information is not available from satellites (e.g., for passive microwave radiometers). Another important issue in synthesis of satellite winds is the partial sampling of different parts of the diurnal cycle by different sun-synchronous satellites that have different local equatorial crossing times. The only exception is the short-term RapidScat measurements currently taking place on the International Space Station (ISS-RapidScat) that was launched in July 2014. The non-sun-synchronous ISS-RapidScat provides the capability to de-alias diurnal variability by cross-calibrating measurements from different sun-synchronous satellites. However, existing synthesis efforts of satellite winds

typically use hourly measurements from buoys such as those from the TAO/TRITON array for that purpose.

In this manuscript we examine and contrast the long term mean and linear trend in two synthesized multi-satellite observed surface wind products. In particular, we examine the two existing versions of the synthesised Cross Calibrated-Multi Sensor (CCMP) data sets [Atlas et al. 2011]. Although the OAflux project also produced a synthesized wind product [Yu and Jin 2012], it was not freely available at the time of research. The length of the CCMP products (1987 onward) makes these products useful for examining multi-decadal changes. As discussed above, the primary motivation for this study is to provide useful information to facilitate the future development of the TPOS. In particular, we analyse the impacts of: i) surface currents on the mean CCMP and TAO/TRITON bias; ii) merging satellite observed relative winds with TAO/TRITON observed absolute winds in CCMP; and iii) background product winds on the mean and longer term trend of the different CCMP versions, as the two versions utilise different background wind products. Perhaps the most important aspect of this paper is our demonstration of the difficulty evaluating the realism/skill of the synthesized winds is a lack of independent in-situ observations to compare against. This difficulty arises as the in-situ data have been assimilated at numerous stages during the generation (i.e., producing the synthesis product background winds and directly in their generation) of the CCMP synthesized satellite wind products. This highlights the need for sensitivity experiments withholding the in-situ data in reanalysis and synthesis surface winds to better understand their true value prior to any proposed observing system changes. This paper is organised as follows. Section 2 details the data sets utilised in this study, while Section 3 details the methods utilised in this study. Results are presented in Section 4 and a discussion and conclusions are presented in Section 5.

2. Data

In this section of the manuscript, the details of all wind and ocean surface current products utilized are presented. We note that each of the presented products employs the oceanographic convention,

meaning a wind blowing toward the Northeast has a positive U component and a positive V component.

TAO/TRITON winds

The TAO/TRITON array is a network of around 70 moored buoys that span most of the tropical Pacific Ocean [McPhaden et al. 2010]. While TAO/TRITON data is archived at sub-daily timescales our analysis uses daily averaged zonal and meridional winds. Wind speed was calculated from this daily averaged data. The quality control flags provided were used to exclude lower-quality or suspect-quality data (i.e., only the highest and default quality data were retained). Combined, missing data and this strict quality control resulted in an average 68% of days (~6000 out of 8766 days) being available for comparison at each location, with a minimum of ~31% in the north western Pacific and a maximum of greater than 90% in the central equatorial Pacific. Wind speed measurements have an accuracy of ±0.3m/s. Measurements are taken at a height of 3.5-4m. These surface winds were adjusted to a height of 10m assuming a neutral buoyancy and logarithmic profile following the method of Atlas et al. [2011], to allow for comparison with the CCMP surface winds.

Cross-Calibrated Multi-Platform (CCMP) surface winds

Daily averaged gridded ocean surface winds, calculated from 6-hourly data, of both the CCMP version 1 [Atlas et al. 2011] and version 2 [Wentz et al. 2015] are utilized here. Both CCMP versions provide the ocean surface winds on a 0.25^{o} latitude and longitude grid. Version 1 covers the period from 2nd July 1987 through until the 31st December 2011, while version 2 continues through until the 30th July 2015. The surface winds are reported at 10m. CCMP winds are created using a variational analysis method (see Atlas et al. 2011 for details), which combines surface winds from satellites, all ship and buoy observations available from NCAR [Atlas et al. 2011], the TAO/TRITON [McPhaden et al. 2010] and PIRATA [Bourles et al., 1998] arrays, along with a background analysis/reanalysis wind product [Atlas et al. 2011]. These background winds are

selected from an analysis or reanalysis product due to their complete space-time coverage, and these winds (provided at 6-hourly intervals) are utilised to provide a first guess of the estimated wind field.

As such, CCMP surface winds reflect the observations available close to the analysis time, while smoothly merging to the background analysis/reanalysis winds where observations are not available. In terms of the proportion of satellite data utilised in the CCMP analysis, Atlas et al. [2011] report that the approximately 25% of the global ocean was observed in a 6-hour window in the late 1980s and this coverage gradually increased to its maximum of approximately 60% in 2000 at the 6-hourly resolution, which has been maintained since. We do not expect major coverage differences between version 1 and version 2 satellite coverage during the overlapping period, given that most of the satellite data used is common to both products. This suggests that in any 6-hour period in the post (pre) 2000 period, CCMP surface winds over approximately 40% (40-80%) of the global ocean are only constrained by the background analysis/reanalysis winds at the 6-hourly resolution. If the data gaps are randomly distributed, this also implies that at any location roughly 40% of the temporally varying data are based on the background analysis/reanalysis winds at that temporal resolution.

Version 1 of CCMP uses the surface winds from ten different satellites, all ship and buoy surface wind observations, including the TAO/TRITON, PIRATA [Bourles et al., 1998] and RAMA [McPhaden et al. 2009] arrays. The background winds are ECMWF operational analysis and ERA-40 reanalysis [Atlas et al. 2011]. It is interesting to note that the ECMWF data switched from reanalysis [Uppala et al. 2005] to analysis [sourced from ECMWF Tropical Ocean and Global Atmosphere global advanced operational surface analysis] at the end of 1998 [Atlas et al. 2011], meaning that background wind source model it is not dynamically consistent in time.

Version 2 of the CCMP winds were created using the same variational analysis method and satellite winds, however, three additional satellite observation sources were incorporated in the more recent period (ASCAT Metop-A, AMSR2, and GMI) to allow for the extension of the data to 2015 (of these, only ASCAT Metop-A provides additional data prior to 2011). In addition, the satellite data utilised in the version 2 synthesis was produced using consistent processing algorithm (RSS version 7 or above) and methodology (unlike version 1), and better quality control on the in situ observations, which also included the TAO/TRITON, PIRATA, and RAMA arrays. Version 2 also updated the background winds, using the higher resolution and consistently produced winds of the continuous 0.25^{o} ERA-Interim reanalysis [Dee et al. 2011].

Background winds

To better understand the role of background wind changes on the differences between the two CCMP products, we also analyse daily averages of the background winds separately. The latter include daily averages (calculated from 6-hourly data) of the, i) CCMP v2 background winds, consisting of the ERA-Interim reanalysis at 0.25^{o} resolution [Dee et al. 2011]; and ii) CCMP v1 background winds, consisting of the ERA-40 reanalysis between the period 1988-1998 [Uppala et al. 2005] and the ECMWF operational analysis for the period between 1999-2011. The ECMWF winds are on a 1.125 degree grid, while the ERA-40 reanalysis winds are available on a 2.5 degree grid. Both the ECMWF and ERA-40 winds are linearly interpolated to a 0.25^{o} grid for the following comparison with CCMP winds.

Satellite surface currents

Here, we also utilise monthly mean surface currents of the Ocean Surface Current Analyses Real-time (OSCAR), which spans the period from October 1992 [Bonjean and Lagerloef, 2002]. The 1° gridded product is used. The OSCAR surface currents, which are representative of the averaged currents over the upper 30m, are computed based on modified geostrophy and Ekman theories from sea surface height (SSH), wind, and temperature [Bonjean and Lagerloef, 2002]. The SSH data are

derived from merged altimeter measurements. The wind products used are from QuikSCAT scatterometer during 1999-2009 and ERA-Interim before and after the QuikSCAT period. Due to the latency of the ERA-Interim product, NCEP operational analysis winds were used for latest few months. This is the only broad-scale product of estimated surface currents available that includes both the geostrophic and Ekman components. However, it is noted that i) the estimated meridional currents do not compare very well with the TAO/TRITON meridional currents where measurements are available [e.g., Johnson et al. 2007], and ii) the average currents in the top 30 m have the potential to be quite different from the currents at the near surface of the ocean [e.g., Cronin and Kessler 2009; Wenegrat and McPhaden 2015]. Satellite winds are relative to the near surface currents, the measurements of which are not available on broad scales even though there are ongoing developments in remote sensing technologies to accomplish this.

3. Methods

3.1 Surface wind comparisons and statistical significance

Firstly, we compare the mean CCMP surface wind data with the mean from TAO/TRITON. When comparing the gridded CCMP data with TAO/TRITON data, we selected the CCMP grid box that encompasses a given TAO/TRITON mooring location. We note that this analysis was carried out only when data from both the TAO/TRITON and CCMP wind data were available. We then seek to understand the role of ocean surface currents in the mean differences between the CCMP products and TAO/TRITON surface winds. To this end, we adjust the CCMP surface winds, which are predominantly satellite observed relative winds, with the OSCAR ocean current estimates to obtain an estimate of absolute winds. This adjustment is done by simply subtracting the zonal and meridional ocean surface current estimate from the corresponding CCMP surface winds.

We also compare both versions of CCMP data on the CCMP grid, and here rather than focusing on surface winds, we focus on the ocean dynamically relevant wind stress, wind stress curl and the y-derivative of wind stress curl [e.g., Kessler 2003]. Wind stresses were calculated from the daily

surface wind data using the quadratic stress law: $(\tau_x, \tau^y) = C_d \rho_a (U,V) W$, where U, V are the zonal and meridional surface wind velocities, respectively, W is the surface wind speed, $\rho_a = 1.2$ kg m^3 is a reference atmospheric density, and $C_d = 1.5x10^{-3}$ is the dimensionless drag coefficient. Wind stress curl (utilised to calculate meridional Sverdrup transport) was calculated using the equation: $curl = \delta\tau^y/\delta y - \delta\tau^x/\delta x$; and both the wind stress curl and its y-derivative (utilised to calculate zonal Sverdrup transport) were calculated using centered differences. The statistical significance of differences in the mean winds and wind stresses in Section 4 of this manuscript were calculated at the 95% level using a two sample t-test with the reduced degrees of freedom as described in Zwiers and Von Storch [1995].

We also compare the linear trends of the CCMP data with TAO/TRITON data, again by selecting the CCMP grid box that encompasses a given TAO/TRITON mooring location and carrying out the analysis only when data from both the TAO/TRITON and CCMP wind data were available. In addition, we carry out a linear trend comparison with both versions of the CCMP data, utilizing the data on the CCMP grid and comparing the ocean dynamically relevant wind stress and its derivatives. The significance of linear trend differences in Section 4.2 of this manuscript was defined when no overlap was found between the trend 95% confidence intervals of the respective linear trends.

3.2 The Linear Shallow Water Model

To better understand the impact of differences in the linear trends of CCMP versions, we use a linear reduced-gravity Shallow Water Model (SWM). The 1 ½ layer SWM is configured on the CCMP 0.25^o grid for the low- to midlatitude Global Ocean between 41^oS–41^oN. The models upper and lower model layers are separated by an interface that represents the pycnocline and applied anomalous wind stresses drive motion in the upper layer, while the lower layer is assumed to be motionless and infinitely deep. These upper-layer dynamics are described by the linear reduced gravity form of the shallow water equations (McGregor et al. 2007; Holbrook et al. 2011). The

model also includes realistic continental boundaries that were calculated as the locations where the bathymetric dataset of Smith and Sandwell [1997] has a depth less than the model mean thermocline (H) of 300 m and a gravity wave speed of 2.8 m s^{-1} is utilized.

4. Results

4.1 Mean differences

We first compare the mean TAO/TRITON surface vector winds and wind speeds with both versions of the CCMP products in an attempt to better understand the differences. Figure 1(a, d, g) displays the mean TAO/TRITON zonal and meridional winds and wind speed, while the difference between the CCMP v1 (CCMP v2) winds and the TAO/TRITON buoy winds is presented in Figure 1b, e, and h (Figure 1 c, f and i). Both CCMP versions display significant mean trade wind differences from the TAO-TRITON winds in some locations, with mean zonal trade winds that are generally too weak in the eastern/central equatorial Pacific and too strong in the north, western and south-western regions of the tropical domain (spatial correlation of 0.90 between CCMP version 1 and 2 spatial biases, Figure 1b and c). Both versions of the CCMP products also display a northward mean meridional wind bias across much of the basin (spatial correlation of 0.80 between Figure 1e and f), which implies overestimated southerly winds in the eastern Pacific and underestimated northerly winds in the western Pacific relative to the TAO/TRITON winds. The CCMP wind speed biases appear to be dominated by the zonal wind biases, which is supported by the spatial correlation -0.97 between the two bias patterns (Figure 1b and h, and Figure 1c and i). Despite the spatial similarity between mean differences of the two versions of the CCMP winds from TAO-TRITON winds, the RMS difference of the CCMP v2 zonal, merdional and wind speed bias is reduced by 25%, 25% and 11%, respectively, compared to CCMP v1 values of 0.26 m s^{-1}, 0.18 m s^{-1}, 0.18 m s^{-1}, which suggests an improvement in the CCMP v2 bias when compared to CCMP v1.

It is clear that these CCMP – TAO/TRITON differences are relatively small compared to the mean winds. This was unsurprising as both CCMP versions are also partially constrained with

TAO/TRITON observations. However, these biases suggest that there are differences in the meridional gradient of the zonal winds, which will likely impact the wind stress curl, and may have significant impacts if this data is used to force ocean model simulations [e.g., Kessler et al. 2003]. Thus, it is important to understand what underlies the differences.

As satellites represent the winds relative to the moving surface ocean (relative winds), it is interesting to examine if the mean surface wind biases can be explained by the ocean surface currents [e.g., Kelly et al. 2001]. Observed estimates of meridional surface currents are very small (Figure 2d) compared to the mean meridional surface wind bias (Figure 1e and f), so have little impact on the overall bias and its significance. The zonal surface currents (Figure 2a), however, have a similar spatial structure (spatial correlation of -0.52 and -0.47 for CCMP versions 1 and 2 respectively) and magnitude to the zonal wind bias's of CCMP v1 and v2 (Figure 1 b and c). By adjusting the CCMP surface winds with the OSCAR ocean current estimates to obtain an estimate of absolute winds, we find that the bias in the equatorial east and south-east have largely changed sign (from too weak to too strong) and in some locations this bias is stronger and more significant than before (Figure 2b and c). There is also a clear weakening of the bias along 5^{o}N, but the bias is still significant in most locations (Figure 2b and c). However, adding a surface current based correction to the CCMP winds has no noticeable effect on the overall CCMP-TAO/TRITON bias (the CCMP v1 and v2 RMS difference remain unchanged at 0.26 m s^{-1} and 0.19 m s-1, respectively). Similarly, there is only a moderate reduction in the bias using corrected CCMP wind estimates (12% and 8% reduction in the RMS difference for CCMP version 1 and 2, respectively). Since OSCAR currents represent the upper 30-m averages, whether the estimates of currents at the very near surface (were they available) would make a larger difference remains to be seen. We are unable to examine whether correction with TAO/TRITON observed 10m surface currents would result in smaller biases as there is limited locations that have this data available for extended durations. Furthermore, it is unclear how the inclusion of the TAO/TRITON measurements in the CCMP surface winds (both directly and through the background reanalysis products) impacts these biases.

However, we could expect that this may act to reduce the difference between the products and this may also lead to an overcorrection in some places when adjusting absolute winds (with ocean surface currents) to relative winds.

It is also interesting to consider the differences between the two CCMP versions on the 0.25^{o} gridded region surrounding the TAO/TRITON array locations and what role the background wind product plays in these differences. Here we focus on evaluating the zonal and meridional wind stresses and wind speed due to their importance for ocean forcing and fluxes, respectively. CCMP version 1 mean equatorial wind stresses are presented in Figure 3 (a, d, and g) along with the version 1 and version 2 difference (version 1 minus version 2) in panels b, e and h. These differences show that the version 2 zonal wind stresses are stronger in the eastern/central Pacific and weaker in the western Pacific. The structure of the meridional wind stress differences show that version 2 wind stresses are more southward in the central basin and more northward to the east and west, but this difference is harder to interpret in terms of the mean. The spatial structure of the wind speed differences are largely consistent with the zonal wind stress differences. We also calculated similar differences between the background products used in each version of CCMP surface winds (Figure 3c, f and i). The spatial agreement between the CCMP differences and the background product differences are clear with spatial correlations of 0.65, 0.75, and 0.62, for the zonal, meridional and wind speed components, respectively. It is also noted that the RMS difference between the CCMP versions zonal stress, meridional stress and wind speeds ($1.9e^{-3}$ Nm^{-3}, $1.1e^{-3}$ Nm^{-3}, and $1.1e^{-1}$ m s^{-1}, respectively) are about 30-40% smaller than the corresponding background product RMS differences. This is likely to be because the background fields are only utilised when satellite observations are lacking.

Calculating the wind stress curl, and the y-derivative of wind stress curl (utilised to calculate zonal Sverdrup transport) from both CCMP versions on their regular grid also reveals distinct differences (Figure 4b and e). Again these differences are largely related to the background wind product

choice (Figure 4c and f), which is reflected by the spatial correlation of 0.79 between Figure 4b and c and 0.60 between Figure 4 e and f. However, the CCMP version differences are relatively small (approximately 1/5 of the magnitude) in comparison to the mean values (Figure 4a and d), which means the zonal Sverdrup transport differences are subtle (Figure 5). Also clear from the differences in CCMP wind stress curl (Figure 4) are the strong positive/negative anomalies straddling most TAO/TRITON locations (denoted by X's) in both the mean and difference plots. These signatures are also evident in the y-derivative of the wind stress curl (which is utilised to calculate zonal Sverdrup transport), which has large localized differences collocated with the TAO/TRITON locations. This is due to the inclusion of the TAO/TRITON data in the CCMP products as it is not apparent in the background wind stress curl (Figure 4c and f). The reason for these spurious curl anomalies may be related to the fact that the TAO/TRITON array absolute winds (measured from a fixed location) are being merged with satellite derived relative winds (relative to a moving ocean surface). This spurious curl in the CCMP versions around the TOA/TRITON locations means that oceanic zonal Sverdrup transport differences (between the two CCMP versions; Figure 5a and c) exhibit differences due to both, the incorporation of localized absolute wind observations (i.e, TAO/TRITON data) and the differing background wind products (Figure 5b and c).

4.2 Long term trends

Here we begin by comparing and contrasting the multi-decadal trends of the CCMP and TAO/TRITON surface wind data over the overlapping period (1988-2011) at common locations. The recent Pacific Trade wind acceleration is clear when examining the linear trend of the TAO/TRITON zonal wind data (Figure 6a, d and g). The zonal wind trend implies an increase in the easterlies by up to 3 m s^{-1} over the 24 year period in the southern and equatorial western Pacific, which at some locations is comparable in magnitude to the mean zonal winds (Figure 1a). Perhaps not surprisingly, as both CCMP versions also incorporate data from the TAO/TRITON array, the changes in zonal and meridional wind components and the surface wind speeds appear to be largely

reproduced in both CCMP versions (Figure 6). As with the mean wind field, more independent information can be obtained by comparing the linear trends of the two CCMP versions in the region surrounding the TAO/TRITON locations. Here we again focus on evaluating the zonal and meridional wind stresses and wind speed due to their importance for ocean forcing and fluxes, respectively.

Again, the recent (1988-2011) trend wind acceleration is clear in the 0.25^{o} gridded equatorial region CCMP data (Figure 7a). The meridional wind stress trend is largely in a northward direction (Figure 7d), consistent with the TAO/TRITON trend (Figure 6d). The wind speed trend largely mirrors the changes in zonal wind stress, except in the east Pacific where meridional winds appear to dominate (Figure 7g). As expected, the equatorial region displays some significant differences between CCMP versions (version 1 minus version 2). Version 2 zonal trends are smaller in the central/eastern Pacific (Figure 7b), where the mean trade winds are stronger (Figure 2b), and larger in the western where the mean trade winds are weaker. The version 2 meridional wind trends are generally smaller south of the equator and larger north of the equator. In terms of wind speeds, version 2 generally has weaker wind speed trends over large parts of the domain. We also calculated the equivalent 1988-2011 trend differences from the background products used in each version of CCMP surface winds (Figure 7c, f and i). The spatial agreement between the CCMP differences and the background product differences is strong, and is summarized by the spatial correlations of 0.89, 0.76, and 0.74, for the zonal, meridional wind stress and wind speed components, respectively. As with the mean state differences, we again find that the RMS difference between the CCMP versions are smaller than those of the background wind products [RMS CCMP zonal stress, meridional stress and wind speed trend differences of 0.004 N m^{-2}, 0.003 N m^{-2}, and 0.22 m s^{-1}, respectively, which are 65%, 66% and 64% of the corresponding background products RMS trend differences].

To assess the importance of these differences for ocean dynamics, we calculate the wind stress curl, y-derivative of the wind stress curl and the zonal Sverdrup transport. It is again clear that the inclusion of the TAO/TRITON data results in spurious wind stress curl anomalies in these derived quantities (Figure 8. a, b, d and e). Again there are large-scale similarities between CCMP version and background wind stress curl differences. However, the spurious curl anomalies introduced around the TAO/TRITON locations reduces the spatial correlation between CCMP curl and CCMP background curl differences (Figure 8b and c; correlation of 0.69), and consequently the CCMP curl y-derivative and the CCMP background curl y-derivative differences (Figure. 8e and f; correlation of 0.44).

To better understand the impact of these wind stress curl changes we forced a linear SWM (described in the Section 3.2) with the two versions of CCMP and CCMP background product wind stress trends to better understand the oceanic impact of these differences and their cause. The CCMP v1 trend generates changes in the equatorial thermocline depth that are up to 25m after 24-years of model integration (Figure 9a). Using the relationship between SWM thermocline depth and sea surface height (SSH) described by Timmerman et al. [2010], this translates to an approximate SSH rise of 7cm over 24-years. The RMS of the CCMP version 1 SWM thermocline depth after 24 years is 14.2m, while CCMP version thermocline differences are up to 5m after 24-years, the RMS thermocline difference is 1.6m (~11% of the magnitude). The accompanying RMS of the version 1 trend surface currents are 2.6 cm s^{-1} zonally and 0.7 cm s^{-1} meridionally after 24 years (Figure 9d and g), while the RMS version 1 and 2 surface current differences are 0.8 cm s^{-1} zonally and 0.4 cm s^{-1} meridionally. Thus, these RMS zonal and meridional current differences are 30% and 55% of the trend magnitudes, respectively. The meridional currents highlight most clearly the impact of the artificial wind stress curl introduced around TAO/TRITON locations, which is most noticeable along 220^{o}E but also apparent elsewhere (Figure 9h) and in the zonal currents (Figure 9e; most notably along 5^{o}N and 220^{o}E). In regards to the role of background state in these changes, the similarity between the CCMP and CCMP background wind forced simulation differences are clear.

This similarity is underlined by spatial correlations between the CCMP and CCMP background product thermocline differences of 0.62, zonal current differences of 0.72 and meridional currents of 0.87. Again highlighting the role of the choice of background wind product in these differences.

4.3 Temporal changes in mean differences

It is also interesting to note that the CCMP mean differences (Figure 3) and the CCMP trend differences (Figure 7) largely mirror each other (spatial correlation of -0.75, -0.55 and -0.44 between the zonal wind stress, meridional wind stress and wind speed respectively). This suggests that the mean difference between products may be getting smaller through the more recent period.

Calculating the mean CCMP version differences in the pre- and post-2000 periods confirms this (Figure 10) as the RMS difference for zonal wind stress, meridional wind stress and wind speed reduces from 0.0029 Nm^{-2}, 0.0017 Nm^{-2}, 0.15 m s^{-1} in the pre-2000 period to 0.0012 Nm^{-2}, 0.0010 Nm^{-2}, 0.1 m s^{-1} in the post-2000 period, respectively. The mean CCMP background version differences during the pre-2000 period (Figure 11a, c and e) reveals spatial patterns that bear many similarities to the corresponding CCMP differences (Figure 10 a, c and e). This spatial similarity is confirmed by high spatial correlations of 0.86, 0.91 and 0.81 between the CCMP and CCMP background pre-2000 mean zonal stress, meridional stress and wind speed, respectively. This suggests that much of the pre-2000 CCMP version differences are due to the choice of background wind product.

In the post-2000 period, however, the differences between the CCMP versions are smaller (Figure 10b, d and f), as are the differences between CCMP version background winds (Figure 11b, d and f). In fact, CCMP background RMS zonal wind stress, meridional wind stress and wind speed difference reduces from 0.004 Nm^{-2}, 0.0023 Nm-2, 0.24 ms-1 in the pre-2000 period to 0.0023 Nm^{-2}, 0.0017 Nm^{-2}, 0.15 ms^{-1} in the post-2000 period (Figure 11). Spatial correlations of 0.28, 0.58 and 0.38 between the CCMP and CCMP background post-2000 mean zonal stress, meridional stress and

wind speed, respectively, indicate that the background winds have a much smaller impact on CCMP versions post-2000. The reduced impact of background products during this most recent period is consistent with both: i) the increased satellite coverage seen during this period [Atlas et al. 2011]; and ii) the smaller differences between background wind products during this period due to improved assimilation and parameterization schemes with the shift to ECMWF analysis. It is noted that the latter point would also benefit from the increased satellite coverage during this period as this data is also assimilated into the reanalysis products. This underlines the importance of sustaining satellite measurements of winds and suggests that if tropical Pacific satellite coverage can be maintained or increased, the impact of background state will be smaller for future trends.

5. Discussion and Conclusions

In this manuscript we have examined two versions of synthesised multi-platform surface winds, the Cross-Calibrated Multi-Platform (CCMP) surface winds, by comparing them with each other and with observed winds from the TAO/TRITON array. This comparison was done to help to inform the future development of the Tropical Pacific Observing System (TPOS), and better understand factors influencing the skill of synthesised satellite wind products in the tropical Pacific. Several studies have been carried out to evaluate the multi-satellite synthesized surface winds and highlighted the skill of these products [Atlas. et al. 2011; Yu and Jin 2012]. However, only time mean skill metrics were evaluated in these previous studies. Here we analyse the impact of: i) surface currents on the mean CCMP and TAO/TRITON bias; ii) merging satellite observed relative winds with TAO/TRITON observed absolute winds in CCMP; and iii) the impact of background product winds on the mean and longer term trend of the different CCMP versions, as the two versions of the CCMP products utilise different background wind products.

The mean differences between the satellite derived CCMP surface winds and those observed from the TAO/TRITON array are relatively small (Figure 1). However, the spatial structure of this bias leads to changes in the meridional gradient of the zonal winds and the wind stress curl, which may have significant impacts on forced ocean model simulations forced with these datasets [e.g., Kessler

et al. 2003]. Thus, it is important to understand the cause of the differences. It is noted that the analysis compares buoy winds at a single location to the gridded data provided by the satellite retrieval averaged over the satellite footprints and it is unclear exactly how this mismatch in scale impacts the comparison. However, it is reasonable to expect that the scale mismatch would only cause smaller-scale, random errors as opposed to large-scale, systematic differences. The similarity between the TAO/TRITON vs CCMP differences and the estimated near-surface currents suggests that the differences are related to the fact that the moored array measures absolute winds while the satellites (the wind data largely utilised in CCMP) measures the wind relative to the moving ocean. This conclusion is consistent with previous studies [e.g., Kelly et al., 2001; Yu and Jin 2012]. Despite this, applying a correction for surface current effects using the OSCAR product (representing top-30m average) does not reduce the overall bias between the mooring and satellite surface winds. It remains unclear whether the lack of improvement is because: i) the uncorrected mooring data has already been assimilated into CCMP; and/or ii) of errors/differences between the OSCAR near surface currents and the actual surface currents [e.g., Johnson et al. 2007]. Also, the fact that the biases are largest under the regions high rainfall bands (e.g., the South Pacific Convergence Zone and the Intertropical Convergence Zone) raises questions about the role of the satellite wind rain contamination [e.g., Milliff et al. 2004; O'Neill et al. 2015; Kilpatrick and Xie 2015] and the background wind data which is used to fill missing data gaps. Clearly, reducing inconsistencies between estimated near-surface currents and wind differences will require: i) direct measurements of currents at the near-surface either using in-situ and satellite platforms; and ii) a better understanding and quantification of the impacts of rain on satellite winds in regions such as the ITCZ and SPCZ across different time scales (e.g., seasonal, interannual, and decadal). These results and uncertainties underline the importance of sustaining in-situ measurements, in particular under the regional rainbands where removal of many moorings is currently proposed as part of TPOS.

The differences in wind stresses and surface wind speeds between the two CCMP versions on the 0.25^{o} grid surrounding the TAO/TRITON locations, while relatively small, have spatial structures that are quantitatively similar to differences between the CCMP background wind products (Figure 3). This highlights the influence of the background wind product choice on the mean state of the synthesized multi-platform winds. This analysis also reveals spurious anomalies in the mean wind stress curl and its y-derivative (used for calculation of zonal Sverdrup transport) at the location of the TAO/TRITON moorings (Figure 4). Similar features are also apparent in the analysis of the multi-decadal trends (1988-2011) of CCMP winds. This suggests that the differences between in situ and satellite surface winds need to be better understood and corrected prior to merging TAO/TRITON winds with satellite observed relative winds.

We also compare the multi-decadal trends (1988-2011) of the CCMP and TAO/TRITON surface wind data to better understand how accurately and consistently these trends are reproduced in the CCMP data. We find that both versions of CCMP winds exhibit trends that are not significantly different from TAO/TRITON at most mooring locations. This may in part stem from the inclusion of the TAO/TRITON winds in the multi-platform product (Figure 6). As with the mean wind field, we compare the trends of the two CCMP versions on the 0.25^{o} grid surrounding the TAO/TRITON locations, to gather more independent information. We find statistically significant differences between the products (Figure 7). These differences have substantial impact on the oceanic response derived from a shallow water model. In particular, the simulated RMS trend differences in the zonal and meridional currents are respectively 30% and 54% of the size of the total trend response (Figure 8 and 9), which would presumably impact SST.

The linear trend differences are largely related to the choice of background wind product. As such, careful consideration is required regarding the most appropriate reanalysis for background state winds as there is considerable differences between the different products in their representation of the mean, annual cycle, interannual variability and longer term trends [e.g., Wittenberg 2004;

McGregor et al. 2012]. This emphasizes the need for enhanced collaboration between the observation and reanalysis communities in improving reanalysis wind products. One important point to note here is that while the CCMP version trend differences are strongly related to differences in the choice of background product, our results also show that the CCMP differences have a smaller magnitude than those of the background products. As such, CCMP products with differing background winds are likely to produce more consistent results when utilized to force ocean models than what might be expected by background (reanalysis) products alone.

We also note that the CCMP mean differences (Figure 3) and the CCMP trend differences (Figure 7) roughly mirror each other and show that the difference between the CCMP versions is significantly reduced during the post-2000 period, when compared to the pre-2000 period. We find that the CCMP version differences in the earlier period are largely related to background wind product choice. In the post 2000 period, however, the differences between the products are smaller and there is a much weaker spatial relationship with the background wind product. Potential causes for the differences between the two periods are: i) the later period has higher rate of global satellite coverage, meaning that the background wind products are utilized less; and ii) the background product for CCMP v1 was also different during this period (see data set description in Section 2.2), and it displayed smaller differences with the CCMP v2 background product. The latter point is likely at least partially related to the former as satellite data is assimilated in the reanalysis. This suggests that if tropical Pacific satellite coverage can be maintained, the impact of background state will be smaller in the future. Conversely, potential future decreases in the tropical Pacific satellite coverage would increase reliance on background state products and give them a greater influence on trend estimates. Therefore, maintaining the current satellite wind measurements should form an important and vital component of TPOS as it can be used to ensure the consistency of reanalysis and synthesized wind products.

In summary, our study identified three important factors that influence the skill of synthesized wind products in terms of mean and trend estimates. The first factor is the quality of the background winds used in the synthesis. To address this issue effectively, enhanced collaborations among the wind observation (both satellite and in-situ) community, reanalysis community, and synthesis community is necessary. The second factor is the need to correct either the satellite-derived relative winds or the in-situ observations of absolute winds prior to synthesizing data sets, such that both are representing the wind from the same perspective. This requires a better understanding of what causes of these wind differences, including the role of ocean surface currents and rain affected satellite retrievals, both of which will be aided by future direct measurements of currents at the very near surface proposed as part of the TPOS. This correction should also lead to enhanced atmospheric reanalysis products. The third factor is that this and previous studies are limited by, is the fact that there is no-independent in-situ data available to evaluate the wind products. This limitation is because the in-situ data have been assimilated in producing atmospheric reanalysis that are used as background winds for the synthesis products (e.g., CCMP and OSCAR), in addition to the use of the in-situ winds in generating the CCMP synthesized satellite wind products. A schematic displaying the current uses of the TAO/TRITON array are presented in Figure 12 to illustrate these measurements are ingrained in the majority of surface wind products. This means that while can state that the differences in CCMP and CCMP background is smaller in the post-2000 compared to the pre-2000 period, we still cannot effectively address whether this recent period is any closer to the in-situ observations. Sensitivity experiments withholding in-situ data in reanalysis and synthesis surface winds are necessary as a first step so that the in-situ winds can be retained for independent validation of the satellite based surface winds, which again points to the need for enhanced collaborations among the observations, reanalysis, and synthesis communities. This independent validation will allow us to better understand the strengths of current observational network and better plan the future changes, and as such should be carried out prior to any diminishment of the current observational network. The current uses of TOA/TRITON data also highlights its true value, as it is utilised as a data source for many wind products and to constrain

and validate numerous others, while also providing the near-real time surface wind data extending back multiple decades (to the arrays formation).

Acknowledgements

The authors acknowledge the TAO Project Office of NOAA/PMEL TAO/TRITON data available (http://www.pmel.noaa.gov/tao/data_deliv/frames/main.html). CCMP Version-2.0 vector wind analyses are produced by Remote Sensing Systems and the data are available at www.remss.com. NASA Physical Oceanography data center, PO.DAAC, is acknowledged for making the CCMP Version-1.0 data (http://podaac.jpl.nasa.gov/Cross-Calibrated_Multi-Platform_OceanSurfaceWindVectorAnalyses) and the OSCAR surface currents available (http://www.esr.org/oscar_index.html). The Asia Pacific Data Research Centre (http://apdrc.soest.hawaii.edu/data/data.php) is acknowledged for making the ERA40 and ECMWF analysis data available, while ECMWF is acknowledged for making the ERA-Interim data available (http://apps.ecmwf.int/datasets/data/interim-full-daily/levtype=sfc/). We would also like to thank the two anonymous reviewers for their helpful comments.

References

Amaya, D. J., S.-P. Xie, A. J. Miller, and M. J. McPhaden (2015), Seasonality of tropical Pacific decadal trends associated with the 21st century global warming hiatus, J. Geophys. Res. Oceans, 120, 6782–6798, doi:10.1002/2015JC010906.

Ando K., T. Matsumoto, T. Nagahama, I. Ueki, Y. Takatsuki, and Y. Kuroda, (2005), Drift Characteristics of a Moored Conductivity-Temperature Sensor and Correction of Salinity Data. J. Atmos. Oceanic Technol., 22 , 282–291, doi:0.1175/JTECH1704.1.

Atlas, R., R. N. Hoffman, J. Ardizzone, S. M. Leidner, J. C. Jusem, D. K. Smith, and D. Gombos (2011), A cross-calibrated, multiplatform ocean surface wind velocity product for meteorological and oceanographic applications, Bull. Am. Meteorol. Soc., 92, 157–174, doi:10.1175/ 2010BAMS2946.1. Available online at http://podaac.jpl.nasa.gov/Cross-Calibrated_Multi-Platform_OceanSurfaceWindVectorAnalyses. [Accessed 25 Nov 2015].

Bonjean, F., and G.S.E. Lagerloef (2002), Diagnostic Model and Analysis of the Surface Currents in the Tropical Pacific Ocean. *J. Phys. Oceanogr.*, **32**, 2938–2954. Available online at ftp://podaac-ftp.jpl.nasa.gov/OceanCirculation/oscar/L4/oscar_1_deg [Accessed 21 Jan 2016].

Bourlès, B., R. Lumpkin, M.J. McPhaden, F. Hernandez, P. Nobre, E. Campos, L. Yu, S. Planton, A. Busalacchi, A.D. Moura, J. Servain, and J. Trotte, 2008: The PIRATA Program: History, Accomplishments, and Future Directions. Bull. Amer. Meteor. Soc., 89, 1111-1125.

Cronin, M.F. and W. S. Kessler (2009), Near-surface shear flow in the tropical Pacific cold tongue front. *J. Phys. Oceanogr.*, **39,** 1200-1215.

Dee, D. P., Uppala, S. M., Simmons, A. J., Berrisford, P., Poli, P., Kobayashi, S., Andrae, U., Balmaseda, M. A., Balsamo, G., Bauer, P., Bechtold, P., Beljaars, A. C. M., van de Berg, L., Bidlot, J., Bormann, N., Delsol, C., Dragani, R., Fuentes, M., Geer, A. J., Haimberger, L., Healy, S. B., Hersbach, H., Hólm, E. V., Isaksen, L., Kållberg, P., Köhler, M., Matricardi, M., McNally, A. P., Monge-Sanz, B. M., Morcrette, J.-J., Park, B.-K., Peubey, C., de Rosnay, P., Tavolato, C., Thépaut, J.-N. and Vitart, F. (2011), The ERA-Interim reanalysis: configuration and performance of the data assimilation system. Q.J.R. Meteorol. Soc., 137: 553–597. doi:10.1002/qj.828. Available online at http://apdrc.soest.hawaii.edu/data/data.php. [Accessed 11 Sep 2015].

England, M. H., S. McGregor, P. Spence, G. A. Meehl, A. Timmermann, W. Cai, A. S. Gupta, M. J. McPhaden, A. Purich, and A. Santoso (2014), Recent intensification of wind-driven circulation in the Pacific and the ongoing warming hiatus, Nature Clim. Change, 4, 222-227.

Holbrook, N. J., I. D. Goodwin, S. McGregor, E. Molina, and S. Power (2011), ENSO to multi-decadal time scale changes in East Australian Current transports and Fort Denison sea level: Oceanic Rossby waves as the connecting mechanism. Deep-Sea Res. II, 58, 547–558, doi:10.1016/j.dsr2.2010.06.007.

Johnson F. Bonjean, G. Lagerloef, J. Gunn, and G. Mitchum, 2007: Validation and Error Analysis of OSCAR Sea Surface Currents, J. Atmos. Oceanic. Technol., 24, 688–701.

Josey, S. A., L. Yu, S. Gulev, X. Jin, N. Tilinina, B. Barnier, and L. Brodeau (2014), Unexpected impacts of the Tropical Pacific array on reanalysis surface meteorology and heat fluxes, Geophys. Res. Lett., 41, 6213–6220, doi:10.1002/2014GL061302.

Kanamitsu, M., W. Ebisuzaki, J. Woollen, S. Yang, J. J. Hnilo, M. Fiorino, and G. L. Potter (2002), NCEP–DOE AMIP-II reanalysis (R-2). Bull. Amer. Meteor. Soc., 83, 1631–1643.

Kelly, K. A., S. Dickinson, M. J. McPhaden, and G. C. Johnson (2001), Ocean currents evident in satellite wind data, Geophys. Res. Lett., 28(12), 2469–2472, doi:10.1029/2000GL012610.

Kessler, W. S., G. C. Johnson, and D. W. Moore (2003), Sverdrup and Nonlinear Dynamics of the Pacific Equatorial Currents, J. Phys. Oceanogr., 33, 994-1008.

Kistler, R., E. Kalnay, W. Collins, S. Saha, G. White, J. Woollen, M. Chelliah, W. Ebisuzaki, M. Kanamitsu, V. Kousky, H. van den Dool, R. Jenne and M. Fiorino, (2001), The NCEP-NCAR 50-Year Reanalysis: Monthly means CD-ROM and documentation. Bull. Amer. Meteor. Soc., 82, 247–267.

Kosaka, Y. and S. P. Xie (2013), Recent global-warming hiatus tied to equatorial Pacific surface cooling, Nature, 501, 403-407.

Kunkee, D. B., G. A. Poe, D. J. Boucher, S. D. Swadley, Y. Hong, J. E. Wessel, and E. A. Uliana (2008), Design and evaluation of the First Special Sensor Microwave Imager/Sounder, IEEE Trans. Geosci. Remote Sens., 46(4), 863–883, doi:10.1109/TGRS.2008.917980.

Lee, T., O. Wang, and W.-Q. Tang, et al. (2008), Wind stress measurements from the QuikSCAT-SeaWinds scatterometer tandem mission and the impact on an ocean model. *J. Geophys. Res.*, 113, C12019, doi:10.1029/2008JC004855.

Lee, T.**,** D.E. Waliser, and J.-L. Li, et al. (2013), Evaluation of CMIP3 and CMIP5 wind stress climatology using satellite measurements and atmospheric reanalysis products. *J. Clim*., 26, 5810-5826, doi:10.1175/JCLI-D-12-00591.1.

McGregor, S., N. J. Holbrook, and S. B. Power (2007), Interdecadal sea surface temperature variability in the equatorial Pacific Ocean. Part I: The role of off-equatorial wind stresses and oceanic Rossby waves. *J. Clim*., 20, 2643–2658.

McGregor, S., Sen Gupta, A. and M. H. England (2012), Constraining wind stress products with sea surface height observations and implications for Pacific Ocean sea level trend attribution. J. Clim. 25, 8164-8176.

McGregor, S., A. Timmermann, M. F. Stuecker, M. H. England, M. Merrifield, F.-F. Jin and Y. Chikamoto (2014), Recent Walker circulation strengthening and Pacific cooling amplified by Atlantic warming, Nature Clim. Change, 4, 222-227.

McPhaden, M. J., A. J. Busalacchi, R. Cheney, J.-R. Donguy, K. S. Gage, D. Halpern, M. Ji, P. Julian, G. Meyers, G. T. Mitchum, P. P. Niiler, J. Picaut, R. W. Reynolds, N. Smith and K. Takeuchi (1998), The Tropical Ocean-Global Atmosphere observing system: A decade of progress, J. Geophys. Res., 103(C7), 14,169–14,240, doi:10.1029/97JC02906.

McPhaden, M. J., S. E. Zebiak, and M. H. Glantz (2006), ENSO as an integrating concept in earth science, Science, 314, 1740–1745, doi: 10.1126/science.1132588.

McPhaden, M.J., G. Meyers, K. Ando,Y. Masumoto, V.S.N. Murty, M. Ravichandran, F. Syamsudin, J. Vialard, L. Yu, and W. Yu, 2009: RAMA: The Research Moored Array for African-Asian-Australian Monsoon Analysis and Prediction. Bull. Am. Meteorol. Soc., 90, 459-480.

McPhaden, M. J., K. Ando, B. Bourlès, H. P. Freitag, R. Lumpkin, Y. Masumoto, V. S. N. Murty, P. Nobre, M. Ravichandran, J. Vialard, D. Vousden, W. Yu (2010), The global tropical moored buoy array. In *Proceedings of the "OceanObs'09: Sustained Ocean Observations and Information for Society" Conference (Vol. 2)*, Venice, Italy, 21–25 September 2009, Hall, J., D.E. Harrison, and D.

Stammer, Eds., ESA Publication WPP-306. Available online at http://www.pmel.noaa.gov/tao/data_deliv/frames/main.html. [Accessed 20 Oct 2015].

Mears, C. A., D. K. Smith, and F. J. Wentz (2001), Comparison of SSM/I and buoy-measured wind speeds from 1987–1997, J. Geophys. Res., 106(C6), 11,719–11,729, doi:10.1029/1999JC000097.

Merrifield, M., (2011), A shift in western tropical Pacific sea level trends during the 1990s. J. Climate, 24, 4126–4138.

Onogi, K., J. Tsutsui, H. Koide, M. Sakamoto, S. Kobayashi, H. Hatsushika, T. Matsumoto, N. Yamazaki, H. Kamahori, K. Takahashi, S. Kadokura, K. Wada, K. Kato, R. Oyama, T. Ose, N. Mannoji and R. Taira (2007), The JRA-25 Reanalysis. J. Meteor. Soc. Japan, 85, 369–432.

Sen Gupta, A., A. Ganachaud, S. McGregor, J. N. Brown, and L. Muir (2012), Drivers of the projected changes to the Pacific Ocean equatorial circulation, Geophys. Res. Lett., 39, L09605, doi:10.1029/2012GL051447.

Sen Gupta, A., S. McGregor, E. van Sebille, A. Ganachaud, J. N. Brown, and A. Santoso (2016), Future changes to the Indonesian Throughflow and Pacific circulation: The differing role of wind and deep circulation changes, Geophys. Res. Lett., 43, doi:10.1002/2016GL067757.

Smith, W., and D. Sandwell (1997), Global seafloor topography from satellite altimetry and ship depth soundings. Science, 277, 1956–1962.

Timmermann, A., S. McGregor, and F. Jin (2010), Wind effects on past and future regional sea level trends in the southern Indo-Pacific. J. Climate, 23, 4429–4437.

Uppala, S. M., P. W. Kallberg, A. J. Simmons, U. Andrae, V. Da Costa Bechtold, M. Fiorino, J. K. Gibson, J. Haseler, A. Hernandez, G. A. Kelly, X. Li, K. Onogi, S. Saarinen, N. Sokka, R. P. Allan, E. Andersson, K. Arpe, M. A. Balmaseda, A. C. M. Beljaars, L. Van De Berg, J. Bidlot, N. Bormann, S. Caires, F. Chevallier, A. Dethof, M. Dragosavac, M. Fisher, M. Fuentes, S. Hagemann, E. Holm, B. J. Hoskins, L. Isaksen, P. A. E. M. Janssen, R. Jenne, A. P. McNally, J. F. Mahfouf, J.-J. Morcrette, N. A. Rayner, R. W. Saunders, P. Simon, A. Sterl, K. E. Trenberth, A. Untch, D. Vasiljevic, P. Viterbo and J. Woollen (2005), The ERA-40 Re-Analysis. Quart. J. Roy. Meteor. Soc., 131, 2961–3012. Available online at http://apdrc.soest.hawaii.edu/data/data.php. [Accessed 16 Jan 2016].

Wenegrat, J.O. and M.J. McPhaden (2015) Dynamics of the surface layer diurnal cycle in the equatorial Atlantic Ocean (0 degrees, 23 degrees W). J. Geophys., Res., 120(1), 563-581, DOI: 10.1002/2014JC010504.

Wentz, F.J., J. Scott, R. Hoffman, M. Leidner, R. Atlas, J. Ardizzone, 2015: Remote Sensing Systems Cross-Calibrated Multi-Platform (CCMP) 6-hourly ocean vector wind analysis product on 0.25 deg grid, Version 2.0, [indicate date subset, if used]. Remote Sensing Systems, Santa Rosa, CA. Available online at www.remss.com/measurements/ccmp. [Accessed 17 Mar 2016].

Wittenberg, A. T., (2004), Extended wind stress analysis for ENSO. J. Climate, 17, 2526–2540.

Yu, L., and X. Jin (2012), Buoy perspective of a high-resolution global ocean vector wind analysis constructed from passive radiometers and active scatterometers (1987–present), J. Geophys. Res., 117, C11013, doi:10.1029/2012JC008069.

Zwiers, and Von Storch (1995), Taking serial autocorrelation into account in tests of the mean, *J. Climate*, **8**, 336-351.

Figure captions:

Figure 1: Time mean TAO/TRITON buoy observed (a) zonal wind, (d) meridional wind and (g) windspeeds. The mean difference between the satellite retrieved CCMP v1 surface zonal wind, meridional wind and windspeed (CCMP v1 minus TAO/TRITON) at each buoy location are respectively presented in (b), (e), and (h), while the mean difference between the satellite retrieved CCMP v2 surface zonal wind, meridional wind and windspeed (CCMP v2 minus TAO/TRITON) at each buoy location are respectively presented in (c), (f), and (i). Locations where the TOA/TRITON and CCMP winds are significantly different (at the 95% level based on a two-sample t-test using the reduced effective degrees of freedom of Zwiers and Von Storch [1995]) are marked with black crosses.

Figure 2: a), d) and g) display the mean OSCAR zonal, meridional and surface current speeds, respectively. Panels b), e) and h) display the CCMP v1 bias's (compared to TAO/TRITON) when the estimated currents are taken into account, while panels c), f) and i) display the CCMP v2 bias's (compared to TAO/TRITON) when the estimated currents are taken into account. Black crosses denote the locations that the CCMP surface winds still have a significant bias regardless of the addition of surface currents, black plus signs are those regions that now display a significant bias with the TAO/TRITON array due to the addition of these currents, while black dashes highlight the regions that the addition of surface currents has acted to remove the significance of the mean bias. Significance is calculated using a two-sample t-test, and determined at the 95% confidence level using the reduced effective degrees of freedom of Zwiers and Von Storch [1995].

Figure 3: The time mean CCMP v1 (a) zonal wind stress, (d) meridional wind stress and (g) wind speeds. The mean difference between the CCMP v1 and CCMP v2 zonal wind stress, meridional wind stress and windspeed (CCMP v1 minus CCMP v2) are respectively presented in (b), (e), and (h), while the mean difference between the CCMP version background wind products zonal wind stress, meridional wind stress and windspeed (CCMP v1 background minus CCMP v2 background) are respectively presented in (c), (f), and (i).

Figure 4: The time mean CCMP v1 (a) wind stress curl, and (g) its y-derivative. The mean difference between the CCMP v1 and CCMP v2 wind stress curl and its y-derivative (CCMP v1 minus CCMP v2) are respectively presented in (b) and (e), while the mean difference between the CCMP version background wind products wind stress curl and its y-derivative (CCMP v1 background minus CCMP v2 background) are respectively presented in (c) and (f).

Figure 5: Mean zonal Sverdrup transports calculated along 160^{o}E from (a) both CCMP versions, (b) both CCMP versions background wind products, and (c) the differences in both.

Figure 6: (a), (d) and (g), respectively, display the long-term (1988-2011) trend in TAO/TRITON bouy zonal wind, merdional wind and windspeed. Statistically significant trends are identified with black X's. (b), (e), and (h) display the difference between the CCMP v1 and TAO/TRITON (CCMP v1 minus TAO/TRITON) zonal wind, meridional wind, and windspeed linear trends, respectively. (c), (f), and (i) display the difference between the CCMP v2 and TAO/TRITON (CCMP v2 minus TAO/TRITON) zonal wind, meridional wind, and windspeed linear trends, respectively. The X's in each of the difference plots indicate linear regression slopes that are significantly different from each other.

Figure 7: The longer-term (1988-2011) linear CCMP v1 linear trend of (a) zonal wind stress, (d) meridional wind stress and (g) wind speed. The mean trend difference between CCMP v1 and CCMP v2 zonal wind stress, meridional wind stress and windspeed (CCMP v1 minus CCMP v2) are respectively presented in (b), (e), and (h), while the mean difference between the CCMP version background wind products zonal wind stress, meridional wind stress and windspeed (CCMP v1 background minus CCMP v2 background) are respectively presented in (c), (f), and (i). Trend

differences that are stippled indicate that there is no overlap between the slope confidence intervals, and thus the differences are deemed significant.

Figure 8: The longer-term (1988-2011) CCMP v1 linear trend (a) wind stress curl, and (g) its y-derivative. The difference between the CCMP v1 and CCMP v2 wind stress curl trend and its y-derivative (CCMP v1 minus CCMP v2) are respectively presented in (b) and (e), while the difference between the CCMP version background wind products linear trend wind stress curl and its y-derivative (CCMP v1 background minus CCMP v2 background) are respectively presented in (c) and (f).

Figure 9: Shallow Water Model (a) thermocline depth, (d) zonal currents and (g) meridional currents after the 24-yr model integration forced by CCMPv1 1988-2011 wind trend. The difference between the CCMP v1 and CCMP v2 trend forced SWM simulations thermocline depth, zonal and meridional currents (CCMP v1 minus CCMP v2) are respectively presented in (b), (e), and (h), while the mean difference between the SWM simulations thermocline depth, zonal and meridional currents differences forced with CCMP version background wind products (CCMP v1 background minus CCMP v2 background) are respectively presented in (c), (f), and (i).

Figure 10: The mean difference between the CCMP v1 and CCMP v2 zonal and meridional wind stress (CCMP v1 minus CCMP v2) in the pre- and post-2000 periods are presented in (a-b) and (c-d), respectively, while the pre and post 2000 mean wind speed differences (CCMP v1 minus CCMP v2) are respectively presented in (e) and (f).

Figure 11: The background product mean difference between the CCMP v1 and CCMP v2 zonal and meridional wind stress (CCMP v1 minus CCMP v2) in the pre- and post-2000 periods are presented in (a-b) and (c-d), respectively, while the background product pre- and post-2000 mean wind speed differences (CCMP v1 minus CCMP v2) are respectively presented in (e) and (f). Note that the CCMP v1 wind stresses during the pre-2000 period are predominantly (prior to 1999) ERA40 surface winds, while the v1 winds post-2000 are ECWMF analysis.

Figure 12: Schematic representation of the products that utilise TAO/TRITON in-situ surface wind observations. Solid lines indicate that the TAO/TRITON data is included in some way in the final product, while dashed arrows indicate that the TAO/TRITON data is used for calibration and validation.

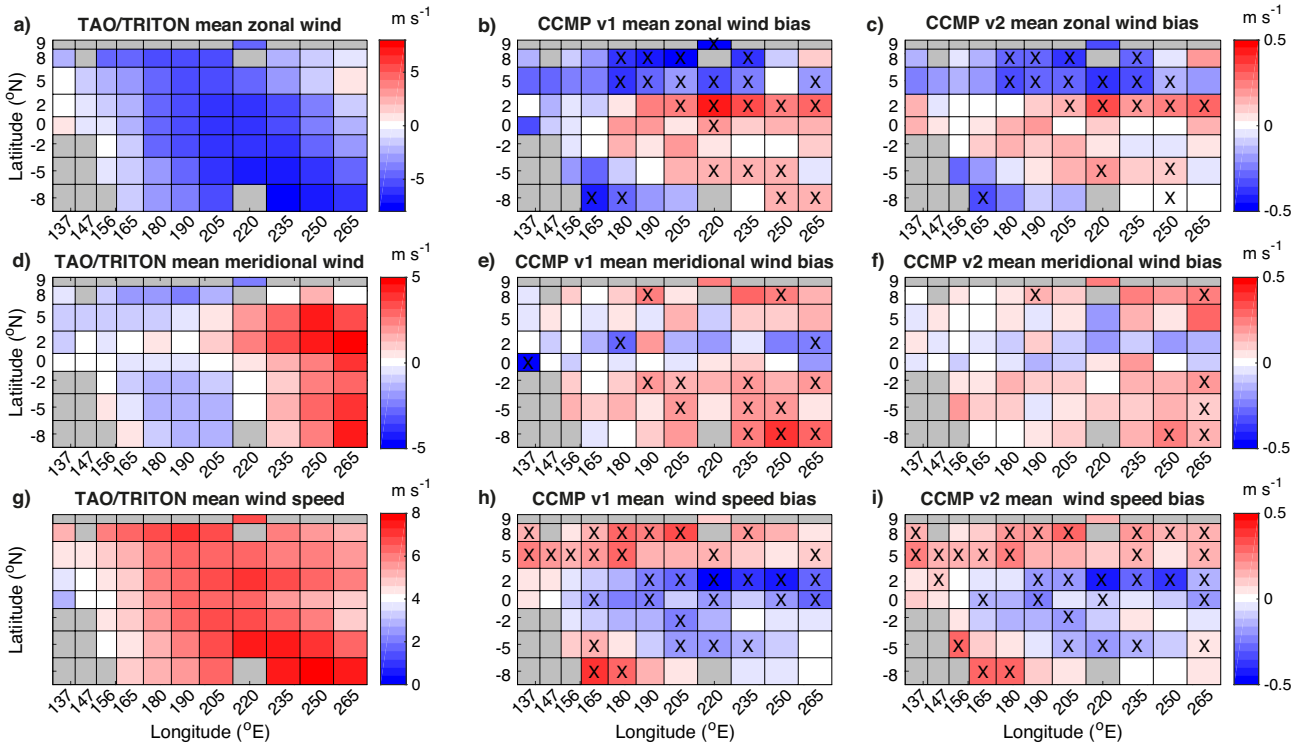

Figure 1: Time mean TAO/TRITON buoy observed (a) zonal wind, (d) meridional wind and (g) windspeeds. The mean difference between the satellite retrieved CCMP v1 surface zonal wind, meridional wind and windspeed (CCMP v1 minus TAO/TRITON) at each buoy location are respectively presented in (b), (e), and (h), while the mean difference between the satellite retrieved CCMP v2 surface zonal wind, meridional wind and windspeed (CCMP v2 minus TAO/TRITON) at each buoy location are respectively presented in (c), (f), and (i). Locations where the TOA/TRITON and CCMP winds are significantly different (at the 95% level based on a two-sample t-test using the reduced effective degrees of freedom of Zwiers and Von Storch [1995]) are marked with black crosses.

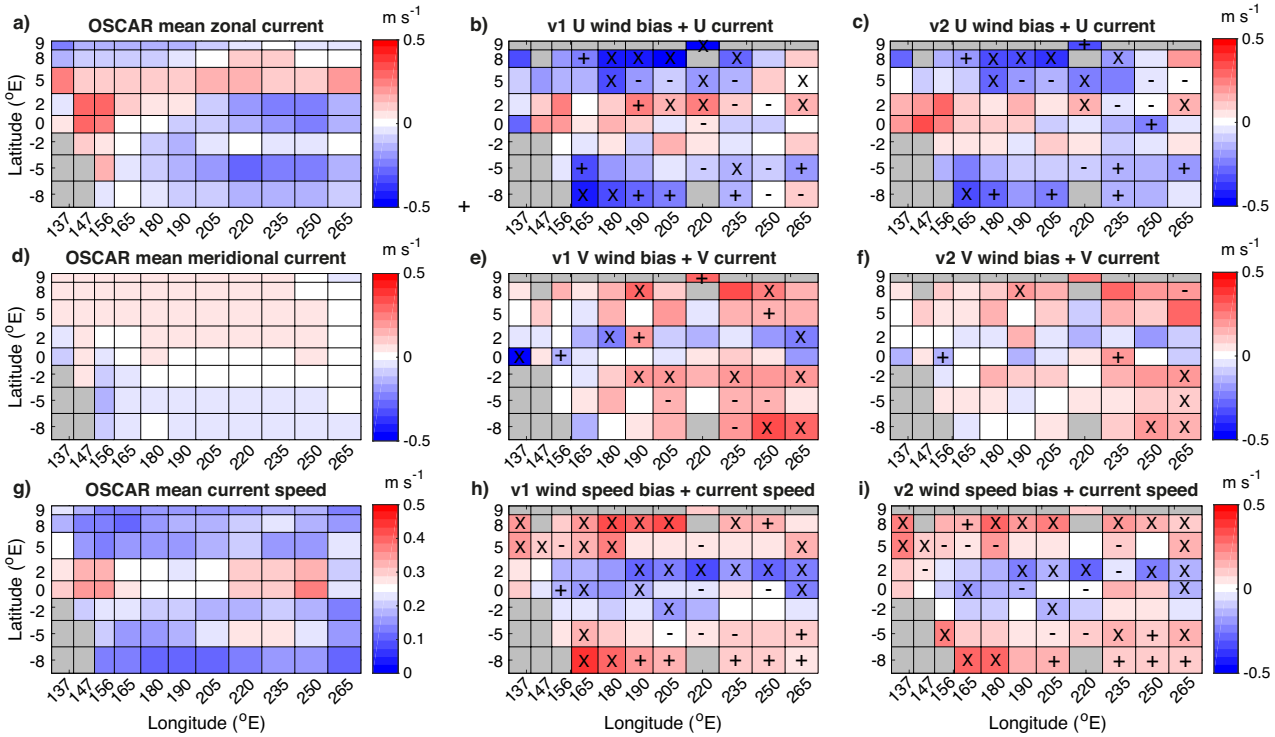

Figure 2: a), d) and g) display the mean OSCAR zonal, meridional and surface current speeds, respectively. Panels b), e) and h) display the CCMP v1 bias's (compared to TAO/TRITON) when the estimated currents are taken into account, while panels c), f) and i) display the CCMP v2 bias's (compared to TAO/TRITON) when the estimated currents are taken into account. Black crosses denote the locations that the CCMP surface winds still have a significant bias regardless of the addition of surface currents, black plus signs are those regions that now display a significant bias with the TAO/TRITON array due to the addition of these currents, while black dashes highlight the regions that the addition of surface currents has acted to remove the significance of the mean bias. Significance is calculated using a two-sample t-test, and determined at the 95% confidence level using the reduced effective degrees of freedom of Zwiers and Von Storch [1995].

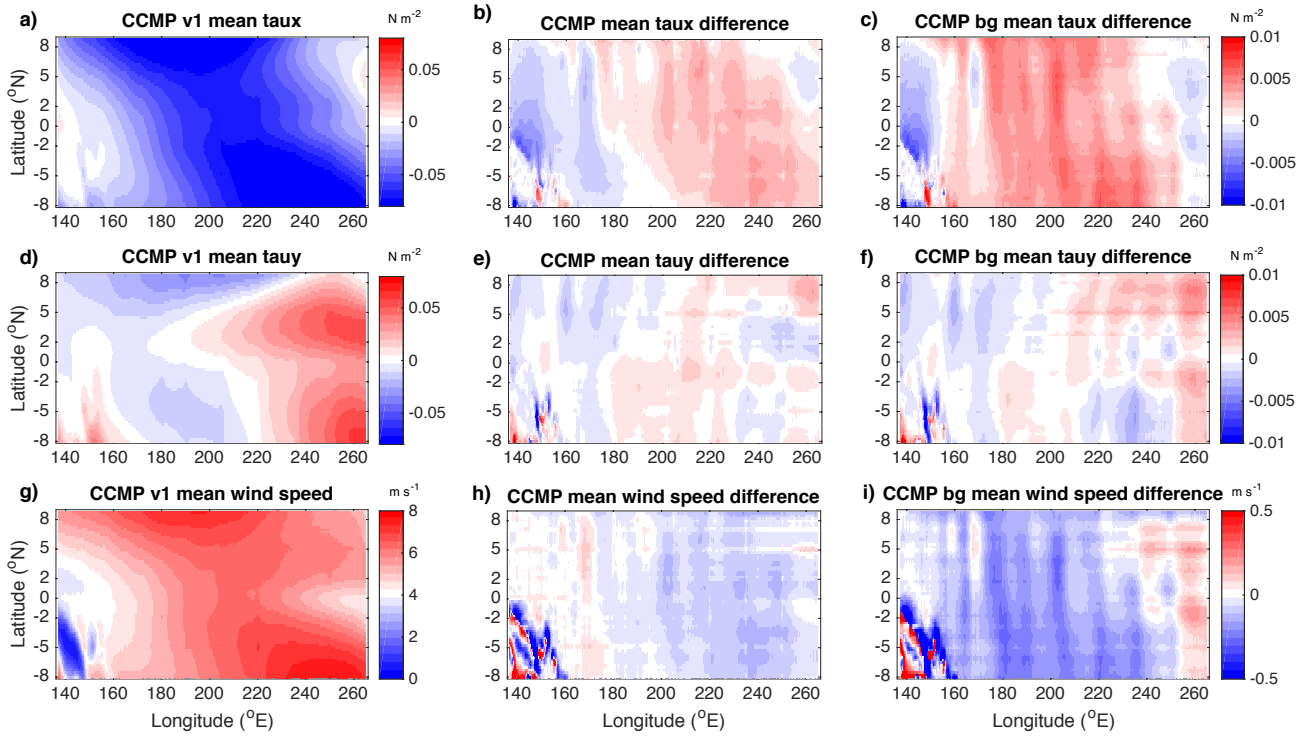

Figure 3: The time mean CCMP v1 (a) zonal wind stress, (d) meridional wind stress and (g) wind speeds. The mean difference between the CCMP v1 and CCMP v2 zonal wind stress, meridional wind stress and windspeed (CCMP v1 minus CCMP v2) are respectively presented in (b), (e), and (h), while the mean difference between the CCMP version background wind products zonal wind stress, meridional wind stress and windspeed (CCMP v1 background minus CCMP v2 background) are respectively presented in (c), (f), and (i).

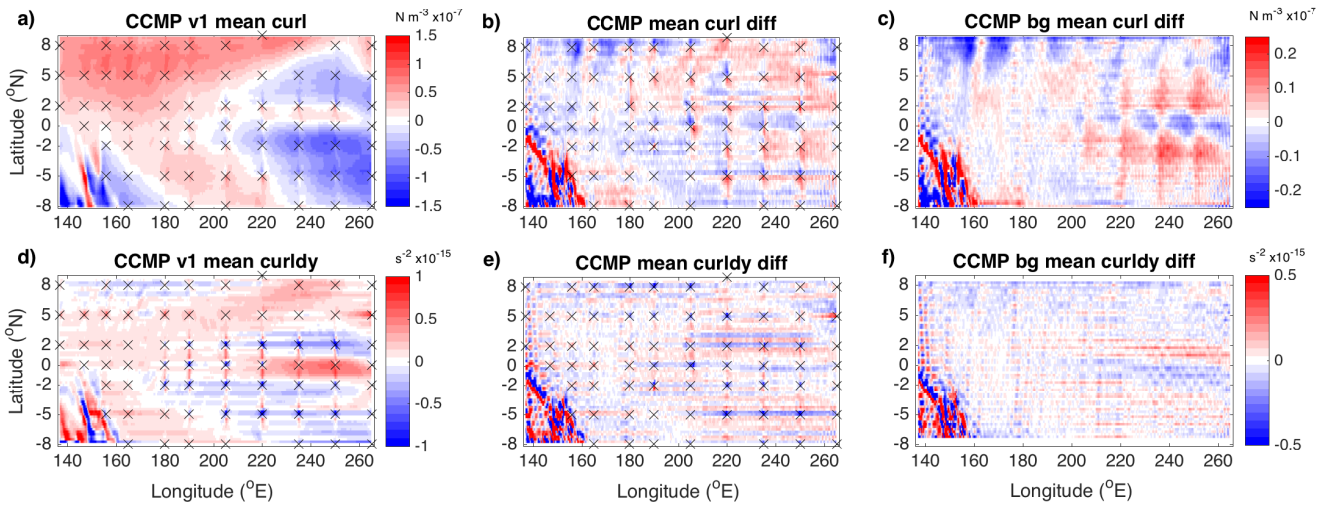

Figure 4: The time mean CCMP v1 (a) wind stress curl, and (g) its y-derivative. The mean difference between the CCMP v1 and CCMP v2 wind stress curl and its y-derivative (CCMP v1 minus CCMP v2) are respectively presented in (b) and (e), while the mean difference between the CCMP version background wind products wind stress curl and its y-derivative (CCMP v1 background minus CCMP v2 background) are respectively presented in (c) and (f).

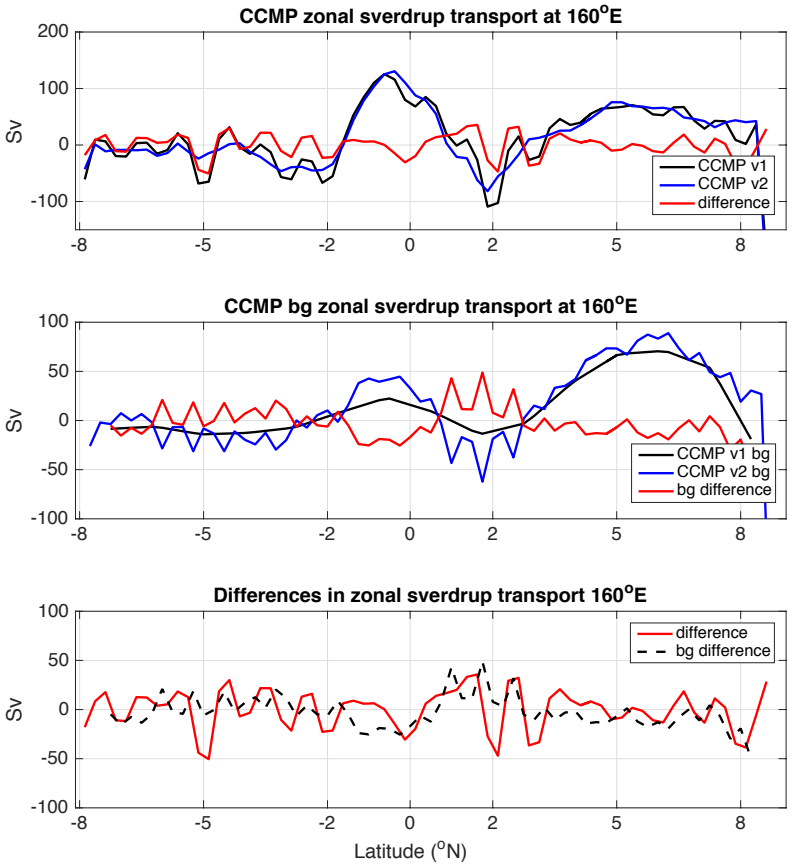

Figure 5: Mean zonal Sverdrup transports calculated along 160°E from (a) both CCMP versions, (b) both CCMP versions background wind products, and (c) the differences in both.

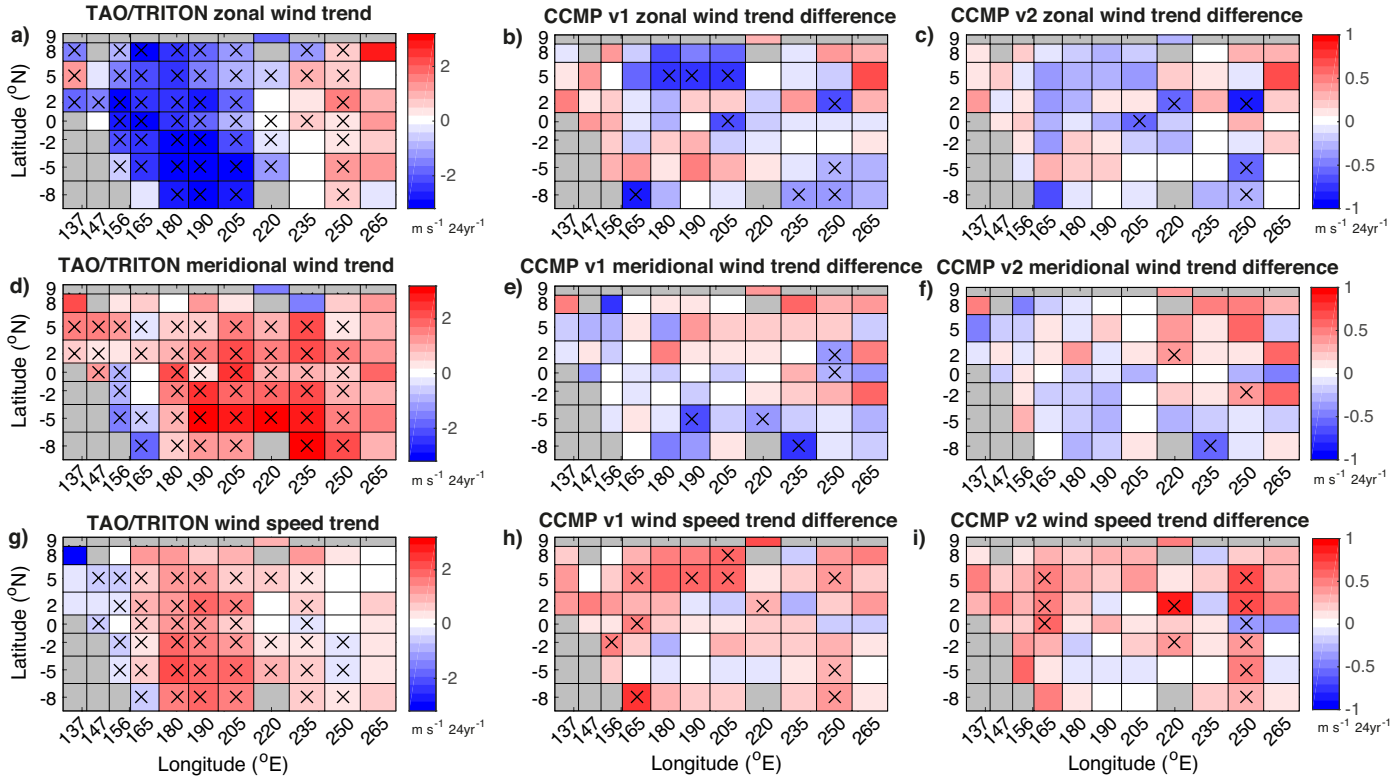

Figure 6: (a), (d) and (g), respectively, display the long-term (1988-2011) trend in TAO/TRITON bouy zonal wind, merdional wind and windspeed. Statistically significant trends are identified with black X's. (b), (e), and (h) display the difference between the CCMP v1 and TAO/TRITON (CCMP v1 minus TAO/TRITON) zonal wind, meridional wind, and windspeed linear trends, respectively. (c), (f), and (i) display the difference between the CCMP v2 and TAO/TRITON (CCMP v2 minus TAO/TRITON) zonal wind, meridional wind, and windspeed linear trends, respectively. The X's in each of the difference plots indicate linear regression slopes that are significantly different from each other.

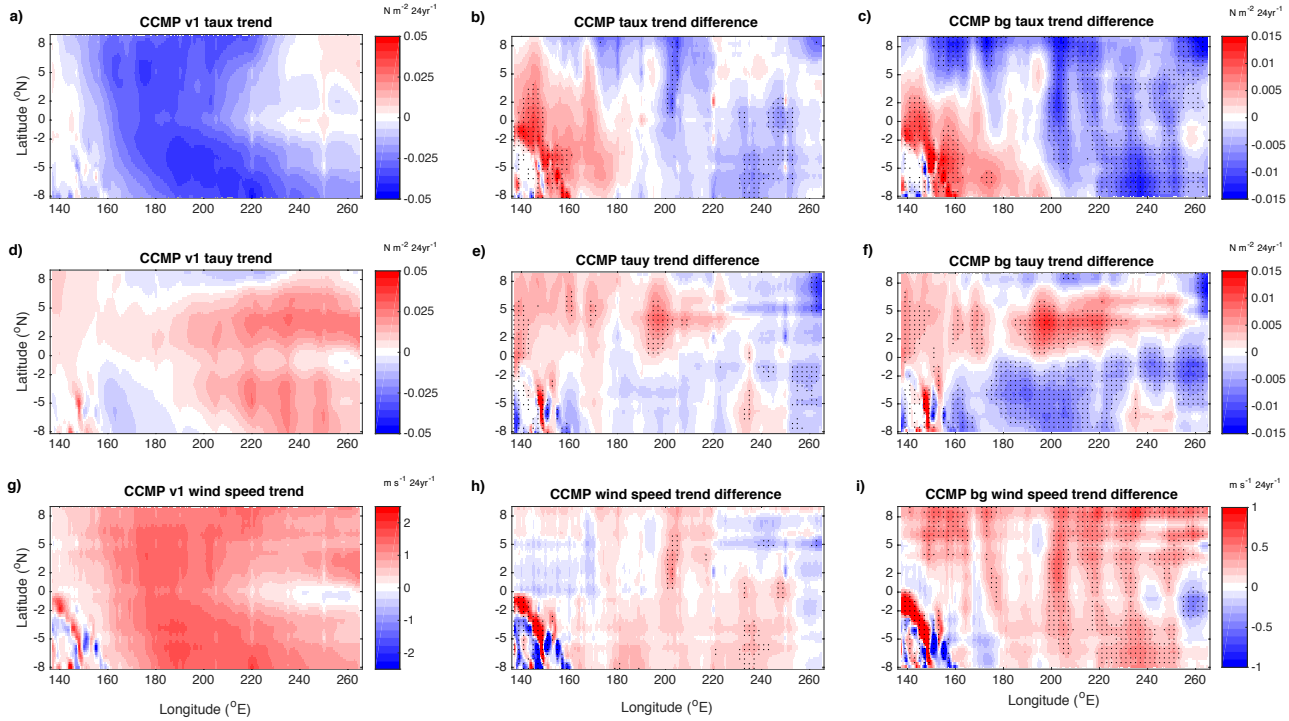

Figure 7: The longer-term (1988-2011) linear CCMP v1 linear trend of (a) zonal wind stress, (d) meridional wind stress and (g) wind speed. The mean trend difference between CCMP v1 and CCMP v2 zonal wind stress, meridional wind stress and windspeed (CCMP v1 minus CCMP v2) are respectively presented in (b), (e), and (h), while the mean difference between the CCMP version background wind products zonal wind stress, meridional wind stress and windspeed (CCMP v1 background minus CCMP v2 background) are respectively presented in (c), (f), and (i). Trend differences that are stippled indicate that there is no overlap between the slope confidence intervals, and thus the differences are deemed significant.

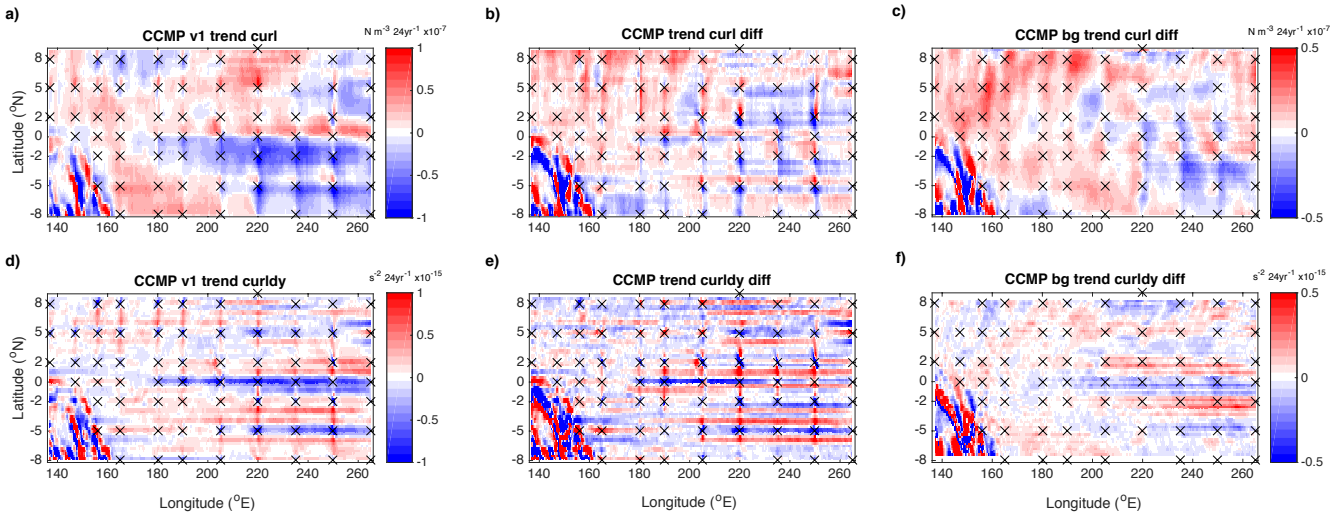

Figure 8: The longer-term (1988-2011) CCMP v1 linear trend (a) wind stress curl, and (g) its y-derivative. The difference between the CCMP v1 and CCMP v2 wind stress curl trend and its y-derivative (CCMP v1 minus CCMP v2) are respectively presented in (b) and (e), while the difference between the CCMP version background wind products linear trend wind stress curl and its y-derivative (CCMP v1 background minus CCMP v2 background) are respectively presented in (c) and (f).

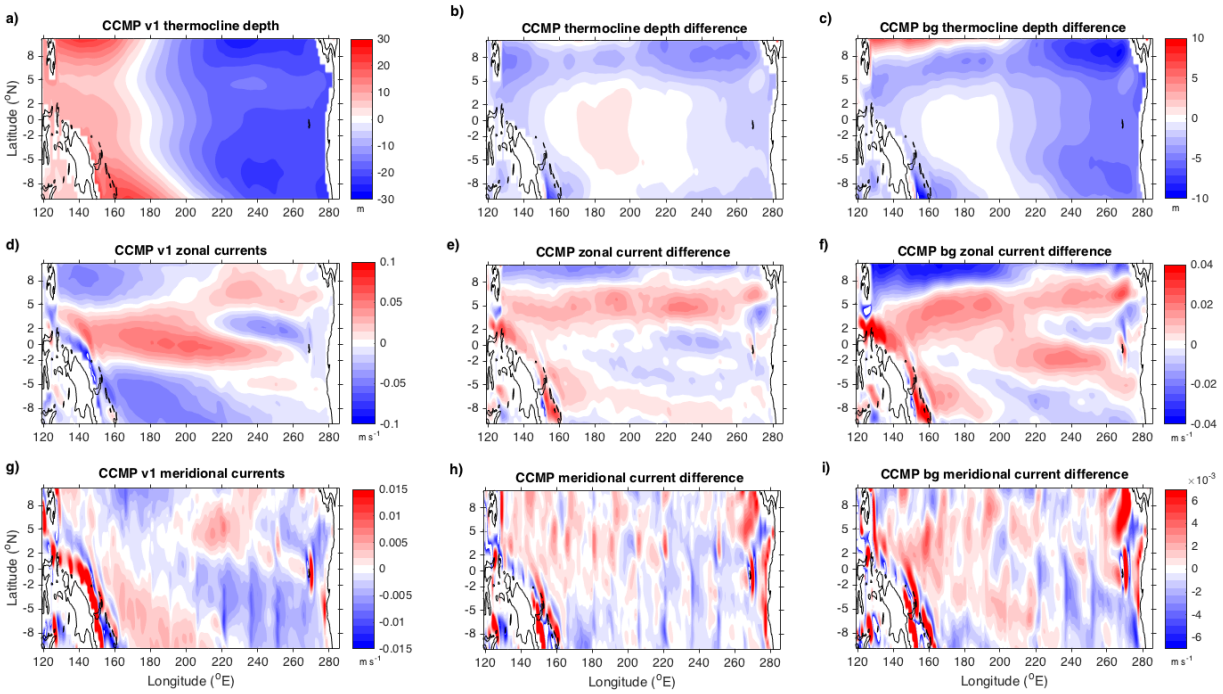

Figure 9: Shallow Water Model (a) thermocline depth, (d) zonal currents and (g) meridional currents after the 24-yr model integration forced by CCMPv1 1988-2011 wind trend. The difference between the CCMP v1 and CCMP v2 trend forced SWM simulations thermocline depth, zonal and meridional currents (CCMP v1 minus CCMP v2) are respectively presented in (b), (e), and (h), while the mean difference between the SWM simulations thermocline depth, zonal and meridional currents differences forced with CCMP version background wind products (CCMP v1 background minus CCMP v2 background) are respectively presented in (c), (f), and (i).

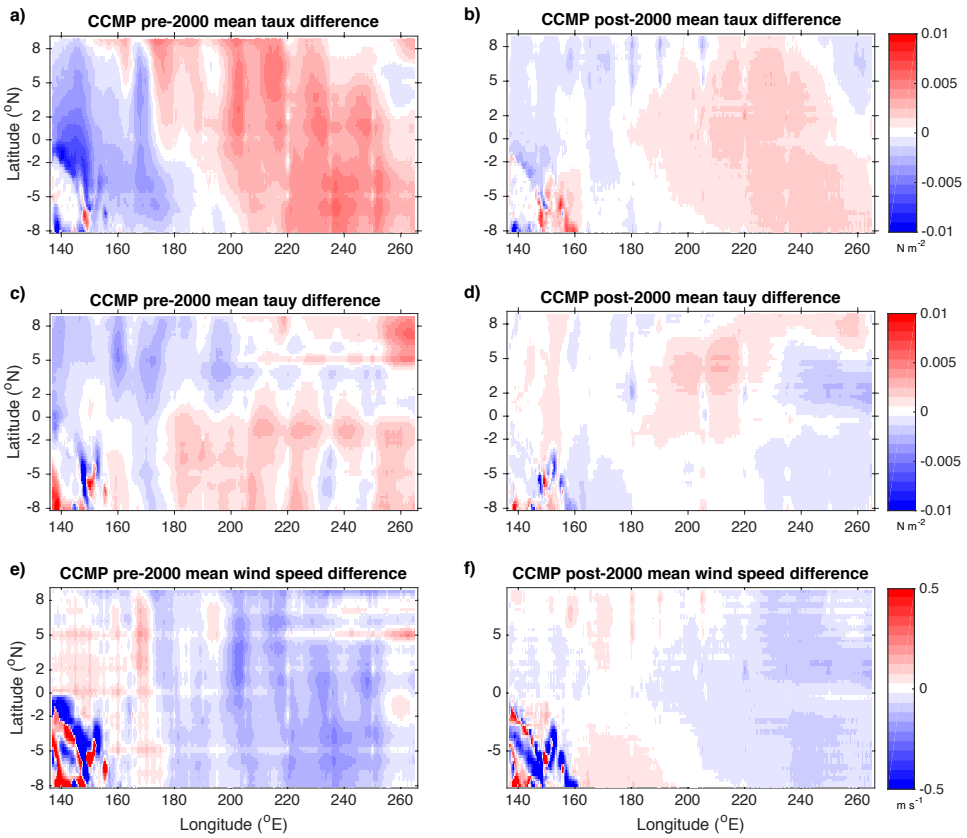

Figure 10: The mean difference between the CCMP v1 and CCMP v2 zonal and meridional wind stress (CCMP v1 minus CCMP v2) in the pre- and post-2000 periods are presented in (a-b) and (c-d), respectively, while the pre and post 2000 mean wind speed differences (CCMP v1 minus CCMP v2) are respectively presented in (e) and (f).

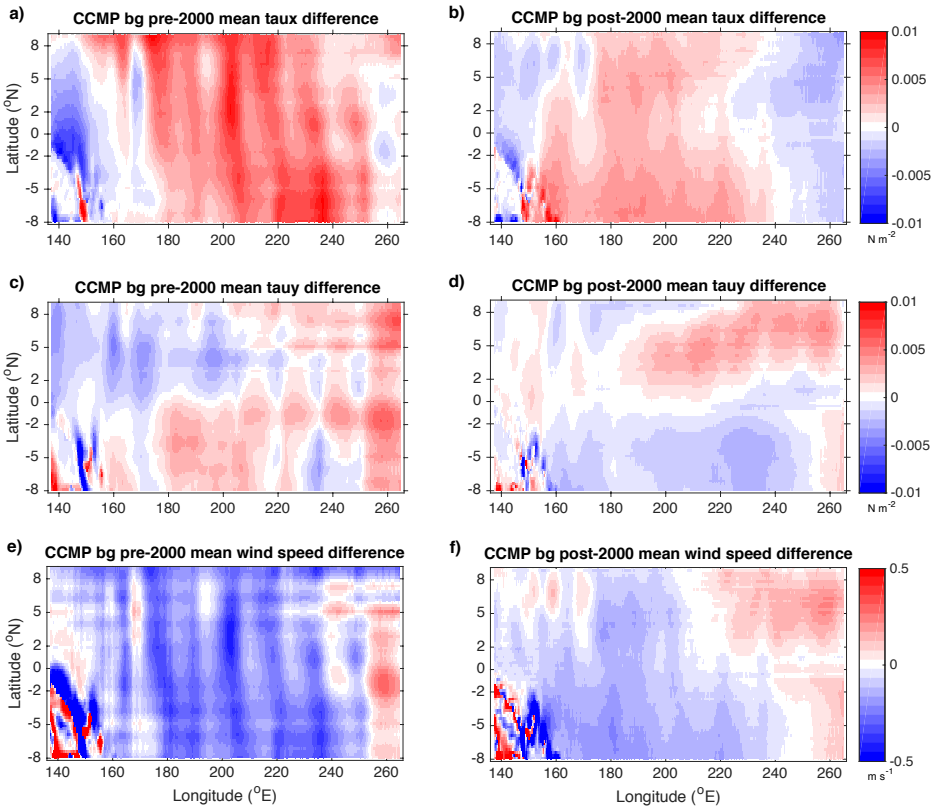

Figure 11: The background product mean difference between the CCMP v1 and CCMP v2 zonal and meridional wind stress (CCMP v1 minus CCMP v2) in the pre- and post-2000 periods are presented in (a-b) and (c-d), respectively, while the background product pre- and post-2000 mean wind speed differences (CCMP v1 minus CCMP v2) are respectively presented in (e) and (f). Note that the CCMP v1 wind stresses during the pre-2000 period are predominantly (prior to 1999) ERA40 surface winds, while the v1 winds post-2000 are ECWMF analysis.

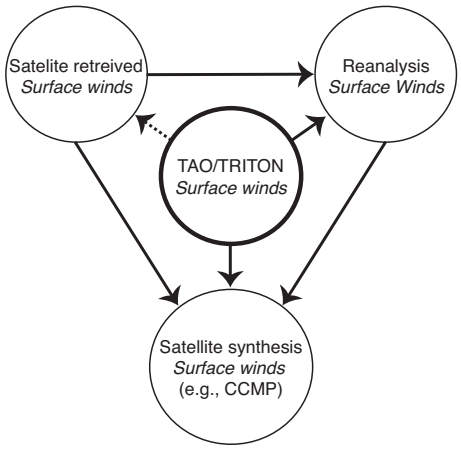

Figure 12: Schematic representation of the products that utilise TAO/TRITON in-situ surface wind observations. Solid lines indicate that the TAO/TRITON data is included in some way in the final product, while dashed arrows indicate that the TAO/TRITON data is used for calibration and validation.